ORIGINAL RESEARCH

NOX1 Promotes Mesothelial–Mesenchymal Transition through Modulation of Reactive Oxygen Species–mediated Signaling

Wenyi Qin, Ann Jeffers, Shuzi Owens, Prashant Chauhan, Satoshi Komatsu, Guoqing Qian, Xia Guo, Mitsuo Ikebe, Steven Idell, and Torry A. Tucker

Department of Cellular and Molecular Biology, The University of Texas Health Science Center at Tyler, Tyler, Texas

Abstract

Pleural organization may occur after empyema or complicated parapneumonic effusion and can result in restrictive lung disease with pleural fibrosis (PF). Pleural mesothelial cells (PMCs) may contribute to PF through acquisition of a profibrotic phenotype, mesothelial–mesenchymal transition (MesoMT), which is characterized by increased expression of α-SMA (α-smooth muscle actin) and other myofibroblast markers. Although MesoMT has been implicated in the pathogenesis of PF, the role of the reactive oxygen species and the NOX (nicotinamide adenine dinucleotide phosphate oxidase) family in pleural remodeling remains unclear. Here, we show that NOX1 expression is enhanced in nonspecific human pleuritis and is induced in PMCs by THB (thrombin). 4-Hydroxy-2-nonenal, an indicator of reactive oxygen species damage, was likewise increased in our mouse model of pleural injury. NOX1 downregulation blocked THB- and Xa (factor Xa)–mediated MesoMT, as did pharmacologic inhibition of NOX1 with ML-171. NOX1 inhibition also reduced phosphorylation of Akt, p65, and tyrosine 216–GSK-3β, signaling molecules previously shown to be implicated in MesoMT. Conversely, ML-171 did not reverse established MesoMT. NOX4 downregulation attenuated TGF-β– and THB-mediated MesoMT. However, NOX1 downregulation did not affect NOX4 expression. NOX1- and NOX4-deficient mice were also protected in our mouse model of *Streptococcus pneumoniae*–mediated PF. These data show that NOX1 and NOX4 are critical determinants of MesoMT.

Keywords: pleural mesothelial cells; pneumonia; nicotinamide adenine dinucleotide phosphate oxidase

Pleural fibrosis (PF) is caused by pneumonia with complicated parapneumonic effusion or empyema, tuberculosis, asbestos-related pleural disease, collagen vascular diseases, or coronary-artery-bypass graft surgery (1–4). Related to pleural infections, the incidence of parapneumonic effusions is increasing and is associated with increased mortality, especially in patients with comorbidities, including pleural loculation and PF (4). PF is promoted by local increments of myofibroblasts, which have been shown to be hyperproliferative and resistant to apoptosis. These cells also actively contribute to the excess deposition of extracellular-matrix proteins such as collagen and fibronectin. Although the sources of these myofibroblasts are not clear, we and others have shown that resident pleural mesothelial cells (PMCs) can differentiate into myofibroblasts though a process called mesothelial–mesenchymal transition (MesoMT). These cells actively contribute to the progression of pleural injury and subsequently contribute to PF (5–8). We previously reported that THB (thrombin), a critical coagulation factor that is represented in pleural injury, induces MesoMT of human PMCs (HPMCs) (7, 8). PI3K/Akt, NFκB, and GSK-3β signaling are important determinants of this process (5, 7). However, the mechanisms by which THB mediates MesoMT have not been fully elucidated.

Oxidative stress is implicated in the pathogenesis of lung and pleural injuries (9–13). NOXs (nicotinamide adenine dinucleotide phosphate oxidases) are important in the generation of reactive

(Received in original form February 28, 2020; accepted in final form January 29, 2021)

Supported by U.S. National Institutes of Health grants HL130133 (T.A.T.) and HL142853 (M.I., S.I., and T.A.T.) and by seed grant funding from The University of Texas Health Science Center at Tyler and The Texas Lung Injury Institute.

Author Contributions: W.Q., A.J., S.O., P.C., S.K., G.Q., X.G., and T.A.T. performed the experiments presented in the manuscript. M.I., S.I., and T.A.T. designed the experiments presented in the manuscript. S.I. and T.A.T. prepared the manuscript. The final version to be published was fully reviewed and approved by all authors.

Correspondence and requests for reprints should be addressed to Torry A. Tucker, Ph.D., The University of Texas Health Science Center at Tyler, 11937 U.S. Highway 271, Biomedical Research Building, Laboratory A-5, Tyler, TX 75708. E-mail: torry.tucker@uthct.edu.

Am J Respir Cell Mol Biol Vol 64, Iss 4, pp 492–503, Apr 2021

Originally Published in Press as DOI: 10.1165/rcmb.2020-0077OC on January 29, 2021
Internet address: www.atsjournals.org

oxygen species (ROS) and subsequent oxidative stress and injury. The family of NOX proteins consists of seven members: NOXs 1–4, NOX4D, NOX5, DUOX1 (NOX6), and DUOX2 (NOX7) (14). Most NOX proteins exist as a combination of subunits requiring at minimum a cytosolic and a membrane-anchoring component. Specifically, NOXs 1–4 are associated with $p22^{phox}$, a transmembrane-based subunit, which anchors the complex to the membrane. Although most members of the NOX family require activation, NOX4 is constitutively active. The principal ROS generated by the NOX family of oxidases are superoxide and H_2O_2. Early NOX studies focused on NOX2-mediated superoxide production, which facilitated killing by phagocytes (14, 15). However, ROS are now known to facilitate and mediate signaling in diverse cell types (16). The prime example is NOX4-mediated ROS, which is reported to play a role in TGF-β–mediated signaling and expression of fibronectin and collagen in the heart, liver, and lung (9, 11, 17–22). Conversely, in vascular smooth muscle cells (23), THB-mediated signaling is in part reported to require NOX1 activation. The contribution of NOX1 to MesoMT has not, to our knowledge, been previously investigated.

Although ROS have been studied in an acute-pleural-injury model (13), the contribution of ROS to subacute pleural injury and PF is not clear. Furthermore, the contribution of the respective NOX family members in MesoMT or PF is unknown. Here, we investigate the role of NOX1 in MesoMT. Our results show that ROS-mediated cellular damage occurs in pleural injury, which coincides with increased coagulation and florid fibrin deposition. NOX1 expression is enhanced in both human and murine pleural injury, suggesting that it may contribute to the pathogenesis of these conditions. We show, for the first time, that NOX1 is induced by Xa (factor Xa) and THB and is a critical mediator of MesoMT.

Methods

Streptococcus pneumoniae–mediated Model of Pleural Injury

All experiments involving animals were approved by the Institutional Animal Care and Use Committee at The University of Texas Health Science Center at Tyler. Pleural instillation of *S. pneumoniae* were performed as previously described (6). C57BL/6 mice, NOX1-deficient mice (24) ($Nox1^{tm1Kkr}$, stock #018787; The Jackson Laboratory), and NOX4-deficient mice ($Nox4^{tm1Kkr}$, stock #022996; The Jackson Laboratory) at 10–12 weeks of age and with a weight ≈ 20 g were lightly anesthetized with isoflurane. Intrapleural inoculations (1.8×10^8 cfu, suspended in 0.9% saline) of *S. pneumoniae* (D39; National Collection of Type Cultures) were delivered in 150 μl of saline by injection as previously described (5, 6).

Lung Histology; Immunostaining; Confocal, Bright-Field Microscopy; and Morphometry

Human pleural tissues (deidentified) were obtained from the National Disease Research Interchange from autopsy specimens from patients with a clinical diagnosis of nonspecific pleuritis. Normal tissues were collected from patients with histologically normal or near-normal pleural tissues that were resected for reasons unrelated to pleural disease or who died of causes otherwise unrelated to any pleural pathologic process. Lung histology and tissue staining were performed as previously described (6, 8, 25). All tissue sections (human and murine) were first deparaffinized and subjected to antigen retrieval using a citrate buffer at 95°C for 20 minutes or an EDTA buffer at 100°C for 10 minutes (for NOX4). Collagen deposition and localization, as well as morphometric changes, were assessed by Trichrome staining, as previously described (8, 25). Pleural tissue thickness and associated pneumonitis were evaluated as we previously described (8). Immunofluorescence was used to visualize 4-hydroxy-2-nonenal (4HNE; HNE11-S; Alpha Diagnostic International) expression in control saline–exposed and *S. pneumoniae*–infected pleuropulmonary sections (5, 8). Normal and pleuritis human tissues were stained for 4HNE, calretinin, NOX1 (SAB4200097; Sigma-Aldrich), and NOX4 (ab133303; Abcam). Differential interference contrast and fluorescence images were collected as previously described (8, 26, 27). Deconvoluted images were generated by "the DeconvolutionLab2" function in ImageJ (National Institutes of Health).

PMC Culture Conditions and Treatment

An exempt protocol, approved by the Institutional Human Subjects Review Board of The University of Texas Health Science Center at Tyler, granted permission to collect and use HPMCs. As previously described (28), HPMCs were isolated from pleural fluids collected from patients with congestive heart failure or from fluids that were post–coronary-bypass pleural effusions. These cells were maintained in LHC-8 culture media (Thermo Fisher Scientific) containing 3% FBS (Thermo Fisher Scientific), 2% antibiotic–antimycotic solution (Thermo Fisher Scientific), and GlutaMAX (Thermo Fisher Scientific), as previously reported (5, 8, 26–29). Cellular characterization using expression of the mesothelial-cell marker calretinin (>95%) was confirmed in all HPMCs before use in experiments.

Quantitative PCR Analyses

Serum-starved PMCs were treated with TGF-β (5 ng/ml; R&D Systems), THB (7 nM; Enzyme Research Laboratory), Xa (7 nM; Enzyme Research Laboratory), uPA (urokinase plasminogen activator; 20 nM; Sekisui Chemical Co., Ltd.), and PLN (plasmin) (7 nM; Molecular Innovations, Inc.). For quantitative PCR (qPCR) analyses, total RNA was isolated from treated cells and transcribed into cDNA as previously described (6, 7). Changes in NOX1, NOX4, and α-SMA (α-smooth muscle actin) gene expression was then determined by qPCR analyses on a Bio-Rad CFX Touch system (Table 1). GUSB was used as the loading control.

Western Blotting

Cell lysates were then Western blotted for α-SMA (MAB1420; R&D Systems), NOX1 (≈72 kD; VPA00110; Bio-Rad), phosphorylated p65 (3033; Cell Signaling Technology), and phosphorylated Akt (4060; Cell Signaling Technology) as previously described (7, 8). β-Actin (A1978; Sigma-Aldrich) was used as the loading control.

NOX Inhibition Studies

For blockade studies, HPMCs were treated with the NOX1 inhibitor ML-171 (10–0.5 μm; Tocris Bioscience) for 18

Table 1. Primer Sequences

Primer	Sequence
NOX1	F: CCGGTCATTCTTTATATCTGTG R: CAACCTTGGTAATCACAACC
NOX4	F: AATTTAGATACCCACCCTCC R: TCTGTGGAAAATTAGCTTGG
ACTA2	Bio-Rad Prime PCR Probe Assay: FAM fluorophore, qHsaCIP0028813
GUSB	Bio-Rad Prime PCR Probe Assay: HEX fluorophore, qHsaCIP0028142

Definition of abbreviations: F = forward; FAM = fluorescein amidite; NOX = nicotinamide adenine dinucleotide phosphate oxidase; R = reverse.

hours in serum-free conditions. Cells were then treated with PBS, THB, or Xa for 24 hours in the presence of ML-171. For reversal studies, serum-starved cells were first treated with THB for 24 hours. ML-171 was then added, and RNA was isolated after 24 hours, whereas proteins were isolated after 48 hours.

For ROS analyses, serum-starved HPMCs were treated with ML-171 (10 μM) for 2 hours in phenol-free RPMI-1640. Cells were then treated with PBS, Xa, and THB for 4 hours. Cells were then incubated with 2′,7′-dichlorofluorescein (10 μM) for 20 minutes and then washed with phenol-free RPMI-1640. Cells were imaged using a Bio-Rad ZOE fluorescent imager. No indications of cytotoxicity were observed with the concentrations of ML-171 used for these studies.

Amplex Red H_2O_2 Measurement

Control cells, siRNA-untransfected cells, and NOX4 siRNA–transfected cells were serum starved and then treated with TGF-β. H_2O_2 generation was then quantified by Amplex Red Hydrogen Peroxide Assay, according to manufacturer's instruction (Thermo Fisher Scientific). Medias Conditioned, Phenol free, serum free media (50 μl) were incubated with the Amplex Red/HRP cocktail in a 96-well plate. The plate was then incubated for 30 minutes at room temperature, and absorbance was measured in a spectrophotometer at 560 nM.

siRNA Transfection

HPMCs were transfected with control siRNA (SIC002), NOX1 siRNA, or NOX4 siRNA (*see* Table 2; Sigma-Aldrich) using Lipofectamine RNAiMAX (Life Technologies Corp.) as previously described (7, 29).

Statistics

All statistics were performed using the Mann-Whitney *U* test or Student's *t* test. A *P* value less than 0.05 was considered to indicate significance.

Results

Characterization of NOX Isoforms in PMCs

To interrogate the role of NOXs in MesoMT, we first characterized NOX expression (NOXs 1–5 and Duoxs 1 and 2) in HPMCs undergoing MesoMT by qPCR analyses. Serum-starved HPMCs were treated with mediators known to induce MesoMT: TGF-β, Xa, THB, PLN, and uPA. The coagulation factors THB and Xa significantly increased NOX1 expression in HPMCs but had little effect on the other NOX family members (Figure 1A). The effect of THB and Xa on NOX1 expression was subsequently confirmed by Western blotting (Figure 1B), as both increased NOX1 expression compared with control HPMCs. NOX4 mRNA expression was potently induced by TGF-β (Figure 1), confirming the results of a previous report (12). TGF-β–mediated increases in NOX4 expression were confirmed by immunofluorescence (Figure 1C). NOX4 expression was not affected by any of the other mediators. NOXs 2, 3, and 5 and DUOXs 1 and 2 were relatively unchanged by treatment with TGF-β, Xa, THB, PLN, or uPA (data not shown). These data show that NOX1 is induced by THB and Xa and likely contributes to MesoMT.

NOX1, NOX4, and 4HNE Expression Is Increased in Pleural Injury

Pleural injury in human cases of nonspecific pleuritis and in our animal models is characterized by increasing numbers of myofibroblasts and increased collagen and α-SMA expression in the remodeled pleural mesothelium (5, 6, 30). Furthermore, we showed that the myofibroblast differentiation of resident PMCs actively contributed to injury progression (5–8, 27). Because NOX1 expression was enhanced by THB and Xa, mediators of MesoMT *in vitro*, we next sought to determine whether NOX1 was, likewise, increased in human PF. We first examined NOX1 expression at the visceral pleural mesothelium of normal human lung tissues and of lung tissues from patients with nonspecific pleuritis. Although NOX1 expression was sparse in normalcy, NOX1 expression was significantly increased at the pleural surface of nonspecific pleuritis tissues (Figure 2A). NOX4 expression was likewise significantly increased in the pleural mesothelium of lung samples from patients with pleuritis compared with normal lung samples (Figure 2B). We also visualized calretinin, a mesothelial-cell marker, to identify the visceral pleurral

Table 2. siRNA Sequences

Gene; siRNA Sequences	siRNA Sequence
NOX1; 1	CUGUUUAACUUUGACUGCU AGCAGUCAAAGUUAAACAG
NOX1; 2	GUUGUUUGGUUAGGGCUGA UCAGCCCUAACCAAACAAC
NOX1; 1	CAGAACAACUCAUAUGGGA UCCCAUAUGAGUUGUUCUG
Negative control (Sigma-Aldrich)	Mission siRNA negative control #2

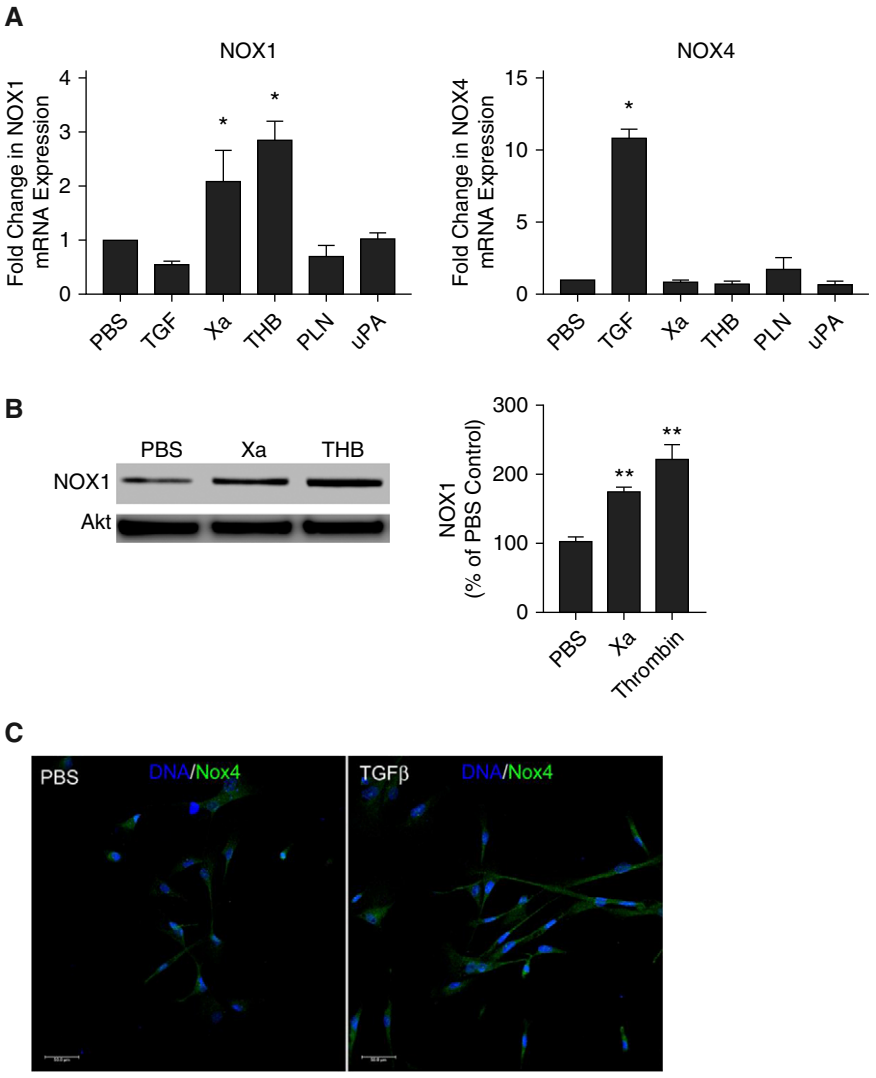

Figure 1. NOX (nicotinamide adenine dinucleotide phosphate oxidase) expression is regulated by mediators of mesothelial–mesenchymal transition (MesoMT). Serum-starved human pleural mesothelial cells (HPMCs) were treated with PBS, TGF-β (5 ng/ml), Xa (factor Xa; 13 nM), THB (thrombin; 7 nM), PLN (plasmin; 7 nM), and uPA (urokinase plasminogen activator; 20 nM) for 24 hours. (*A*) RNA was then isolated, transcribed into cDNA, and then analyzed for NOX expression by quantitative PCR (qPCR). Data are expressed as means ± SEMs and represent three to six samples per condition. (*B*) NOX1 expression in PBS-, Xa-, and THB-treated cells was determined by Western blotting. Akt was used as the loading control. Xa- and THB-treated cells demonstrated increased NOX1 expression. The blots are representative of three independent experiments. (*C*) NOX4 expression (green) and nuclei (blue) were imaged in PBS- and TGF-β–treated HPMCs by immunofluorescent microscopy. Images show 25× magnification and are representative of the findings of three samples per treatment and 10 fields per slide. Scale bars, 50.0 μm. $^{*}P < 0.05$ compared with PBS controls. $^{**}P < 0.01$ compared with PBS controls. TGF = transforming growth factor.

mesothelium in these samples (Figure 2C).

Because oxidative stress has been shown to contribute to pleural injury in an acute mouse model of pleural injury (13) and NOXs 1 and 4 were increased in pleural injury, we next sought to determine whether ROS-mediated damage was present in our empyema model of PF. 4HNE was measured on the surface of empyema-injured mouse lung tissues via immunofluorescent staining. 4HNE, primarily the result of β-oxidation–pathway metabolization of lipid peroxides, can serve as an indicator of ROS-dependent tissue damage. In Figure 3, we show that 4HNE staining was significantly increased in tissues with empyema-mediated pleural injury at 3, 7, and 14 days compared with saline treated control animals (14 d). Furthermore, 4HNE appeared to be limited to the pleural surface of injured mice and progressively increased throughout the 14-day time course. 4HNE was not detected in control mice.

NOX1 Is Critical for the Induction MesoMT

Because NOX1 expression was enhanced in human pleuritis and upregulated by Xa and THB, we next investigated the role of NOX1 in MesoMT. We first confirmed that NOX1 expression was significantly reduced by siRNA transfection compared with PBS and THB treatment (Figure 4A, $P < 0.05$). Next, untransfected, control siRNA–transfected, and NOX1 siRNA–transfected cells were treated with THB. Although THB treatment induced α-SMA in untransfected and control siRNA–transfected cells (Figure 4A), NOX1-downregulated cells demonstrated induction of α-SMA when treated with THB. qPCR analyses of NOX1-downregulated cells (>80%, $P < 0.05$) showed similar results (Figure 4B). These findings were confirmed with a second NOX1 siRNA (data not shown). These studies show that NOX1 is critical for THB- and Xa-induced MesoMT. Similar results were observed with Xa, as NOX1 knockdown ($P < 0.05$) blocked Xa-mediated induction of α-SMA (Figure 4C).

NOX1 Inhibition Attenuates MesoMT

Because NOX1 downregulation significantly attenuated the induction of MesoMT, we next studied the effect of small-molecule inhibition of NOX1 on THB-mediated MesoMT. ML-171 in varying concentrations (10–1 μM) was used to inhibit NOX1 activity before the addition of THB. ML-171 (10–2 μM) significantly blocked THB-mediated α-SMA induction ($P < 0.05$, Figure 5A). Induction of fibronectin was likewise blocked by all doses of ML-171. We next determined the effect of NOX1 inhibition on signaling pathways previously shown to be critical in MesoMT (5, 7). THB-mediated phosphorylation of Akt, NFκB (p65), and GSK-3β (tyrosine-216) were reduced by ML-171. The effect of ML-171

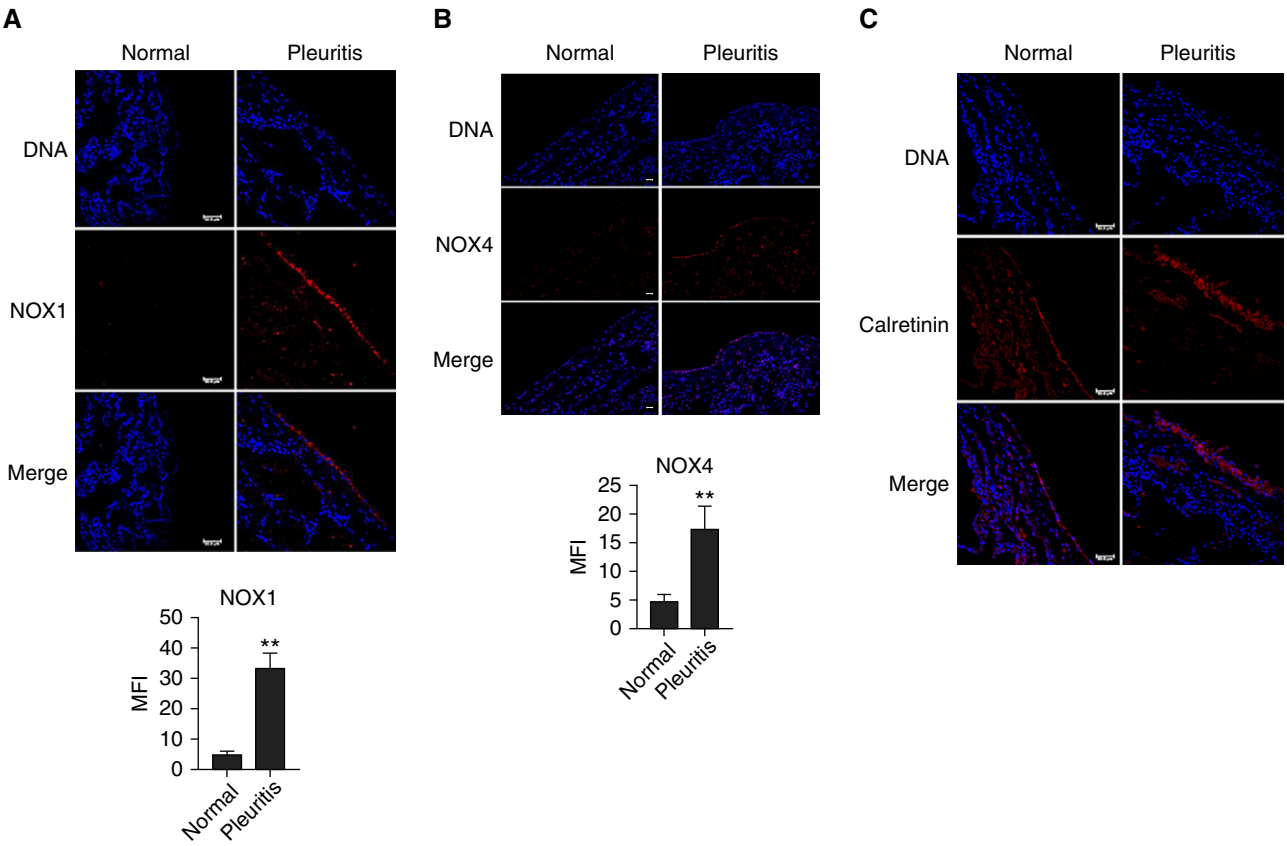

Figure 2. NOX1 and NOX4 expression is enhanced in human nonspecific pleuritis. Lung-tissue sections from patients with diagnosed nonspecific pleuritis were immunofluorescently labeled. (*A*) NOX1 expression (red) was increased at the pleural surface of the nonspecific pleuritis tissue. NOX1 expression was not detected in normal pleural tissues. Scale bars, 50.0 μm. (*B*) NOX4 expression (red) was increased at the pleural surface of the nonspecific pleuritis tissue. NOX4 expression was detected normal pleural tissues. (*C*) Calretinin expression (red) was localized to the pleural surface of normal and pleuritis tissue sections. Images show 25× magnification and are representative of the findings of 30 fields per slide and three to four patients per group. Scale bars, 50 μm. $^{**}P < 0.01$ compared with nonspecific pleuritis. MFI = mean fluorescence intensity.

on induction of the MesoMT marker α-SMA was confirmed by qPCR analyses (Figure 5B), showing that ML-171 attenuated THB-mediated MesoMT. ML-171 also reduced THB-mediated induction of NOX1 but did not alone reduce NOX1 expression below control levels. Similar results were observed with Xa (Figure 5C) and TGF-β (Figure 5D), as the highest doses of ML-171 (10 and 5 μM) blocked induction of MesoMT markers and attenuated signaling.

We next evaluated the effectiveness of NOX1 inhibition in established MesoMT. For these studies, serum-starved HPMCs were treated with THB for 24 hours before the addition of the NOX1 inhibitor (ML-171, 5–1 μM). Cells were then incubated for another 24 hours. Unlike the previously described blockade studies, no concentration of ML-171 demonstrated any reduction in THB-mediated increases in α-SMA (Figure 5E). Furthermore, AKT and p65 phosphorylation was not affected when the inhibitor was used after the initiation of MesoMT. Conversely, fibronectin expression was attenuated by ML-171 in these analyses. qPCR analyses, performed in parallel, showed similar results (data not shown). These studies show that although NOX1 inhibition with ML-171 can block the progression of MesoMT, the inhibitor did not reverse established MesoMT apart from limiting fibronectin expression.

The role of NOX1 in Xa and THB-mediated ROS generation was next evaluated (Figure 5F). Although Xa and THB significantly increased ROS generation in HPMCs ($P < 0.05$), the NOX1 inhibitor ML-171 reduced ROS-mediated fluorescence to baseline levels. These studies strongly suggest that initiation of Xa and THB-mediated ROS generation is NOX1 dependent.

NOX1 Downregulation Attenuates TGFβ-mediated MesoMT

TGF-β is widely considered to be the "gold standard" of profibrotic mediators because of its ability to induce myofibroblast differentiation in numerous cell types, including HPMCs. Furthermore, the NOX1 inhibitor ML-171 blocked TGF-β-mediated MesoMT. As such, we extended our evaluation of NOX1 to TGF-β mediated MesoMT. Like THB, TGF-β–mediated induction of α-SMA protein was attenuated by NOX1 downregulation (Figure 6A). These results were consistent with the responses observed by qPCR analyses (data not shown). These data suggest that the role

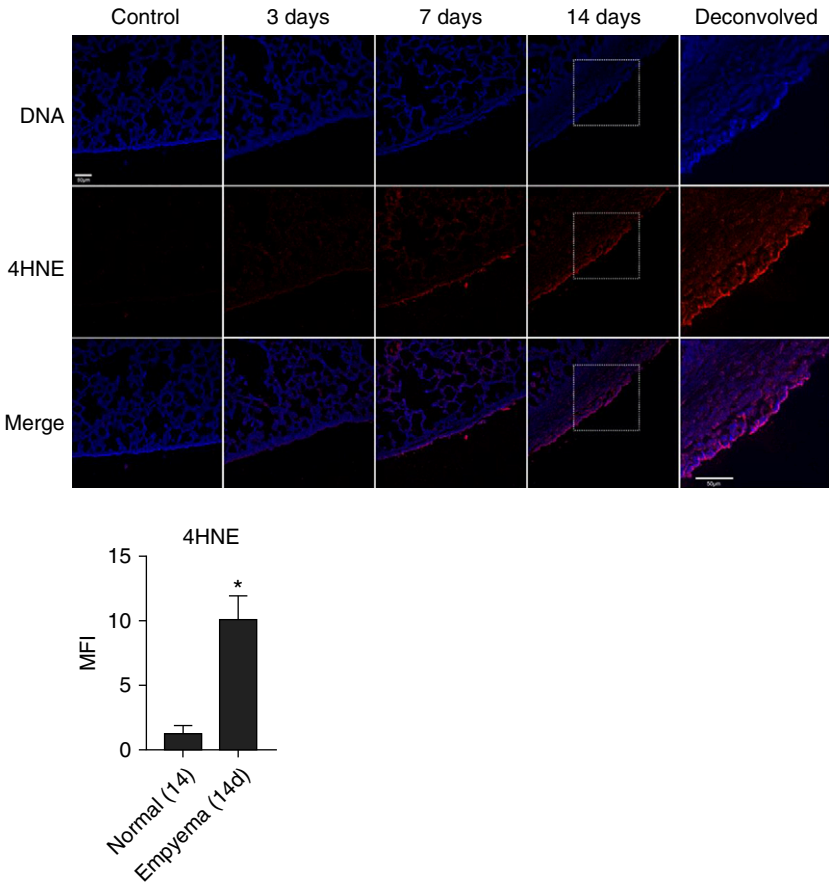

Figure 3. 4-Hydroxy-2-nonenal (4HNE) is increased in murine empyema. Lung-tissue sections from normal and empyema-injured mice were immunofluorescently labeled. 4HNE expression (red) was increased at the pleural surface of empyema-injured mice (at 3, 7, and 14 d). Images show 25× magnification and are representative of the findings of 30 fields per slide and three to four mice per group. Deconvolved images at a higher magnification are shown in the boxed areas in the 14-day tissue section. Scale bars, 50 μm. *$P < 0.05$ compared with normal controls.

of NOX1 is common to THB- and TGF-β–mediated MesoMT.

NOX4 is a critical mediator of TGF-β–dependent myofibroblast differentiation in diverse cell types (9, 11). However, studies in HPMCs have been limited (12). Because TGF-β induced NOX4 expression in our HPMCs, we next determined the contribution of NOX4 to TGF-β mediated MesoMT. NOX4 downregulation by siRNA significantly attenuated TGF-β–mediated induction of α-SMA in HPMCs compared with untransfected and control siRNA–treated cells (Figure 6B). Akt and GSK-3β phosphorylation was also reduced in NOX4-downregulated HPMCs. NOX4 downregulation was quantified by qPCR (>80%, Figure 6C). Because NOX1 downregulation likewise attenuated TGF-β–mediated MesoMT, we next determined the effect of NOX1 downregulation on TGF-β–mediated changes in NOX4 expression. Although NOX1 was significantly reduced by NOX1 siRNA, neither baseline nor TGF-β–induced NOX4 expression was affected by NOX1 downregulation (Figure 6D). Similar results were found with Xa (Figure 6E) and THB (Figure 6F), as NOX4 downregulation significantly blocked induction of α-SMA and Akt phosphorylation ($P < 0.05$). These results show that induction of MesoMT is dependent on both NOX1 and NOX4 expression. Furthermore, these studies suggest a synergy between NOX1 and NOX4 in the induction of MesoMT.

NOX1 and NOX4 Deficiency Reduced *S. pneumoniae*–mediated PF

Because downregulation of NOX1 and NOX4 expression and function blocked the induction of MesoMT, we next determined the role of NOX1 and NOX4 in the progression of PF *in vivo*. Wild-type (WT), NOX1-deficient, and NOX4-deficient mice were intrapleurally injected with *S. pneumoniae* over a 7-day time course. Figure 7A shows that *S. pneumoniae*–mediated pleural injury was associated with significant decrements in lung function (compliance, $P = 0.0079$) and reduced lung volume ($P = 0.03$) compared with saline treatment in WT mice. Conversely, *S. pneumoniae*–mediated pleural injury did not significantly change lung volume or function in NOX1- or NOX4-deficient mice when compared with control animals. Histologic analyses of lung-tissue sections showed significantly increased pleural thickening in *S. pneumoniae*–injured WT mice (Figure 7B). However, NOX1- and NOX4-deficient mice demonstrated significantly less pleural thickening ($P = 0.03$ and $P < 0.05$, respectively) than similarly treated WT mice.

Discussion

In this study, we sought to characterize the contribution of the NOX family of proteins to the phenotypic differentiation of HPMCs to myofibroblasts and to PF after empyema. We first found that THB and Xa, mediators of MesoMT, preferentially induce NOX1 expression in HPMCs. Furthermore, NOX1 expression was enhanced in human pleuritis and murine pleural injury. We also provide evidence of ROS-mediated injury in our empyema model. Second, we identified a novel role for NOX1 in the myofibroblast differentiation of HPMCs. Although Nox4 has been implicated in myofibroblast differentiation of diverse cell types, its role and that of other NOXs in MesoMT has heretofore been unknown. Our data clearly show that inhibition of NOX1 can attenuate MesoMT. To our knowledge, this represents the first evidence that NOX1 is a critical determinant of MesoMT.

We first characterized the expression of NOX family members in HPMCs using known mediators of MesoMT. Of the seven NOX isoforms we tested, only two were found to be modulated by mediators of MesoMT, NOX1 and NOX4. As previously reported, we found that TGF-β significantly induced NOX4 expression

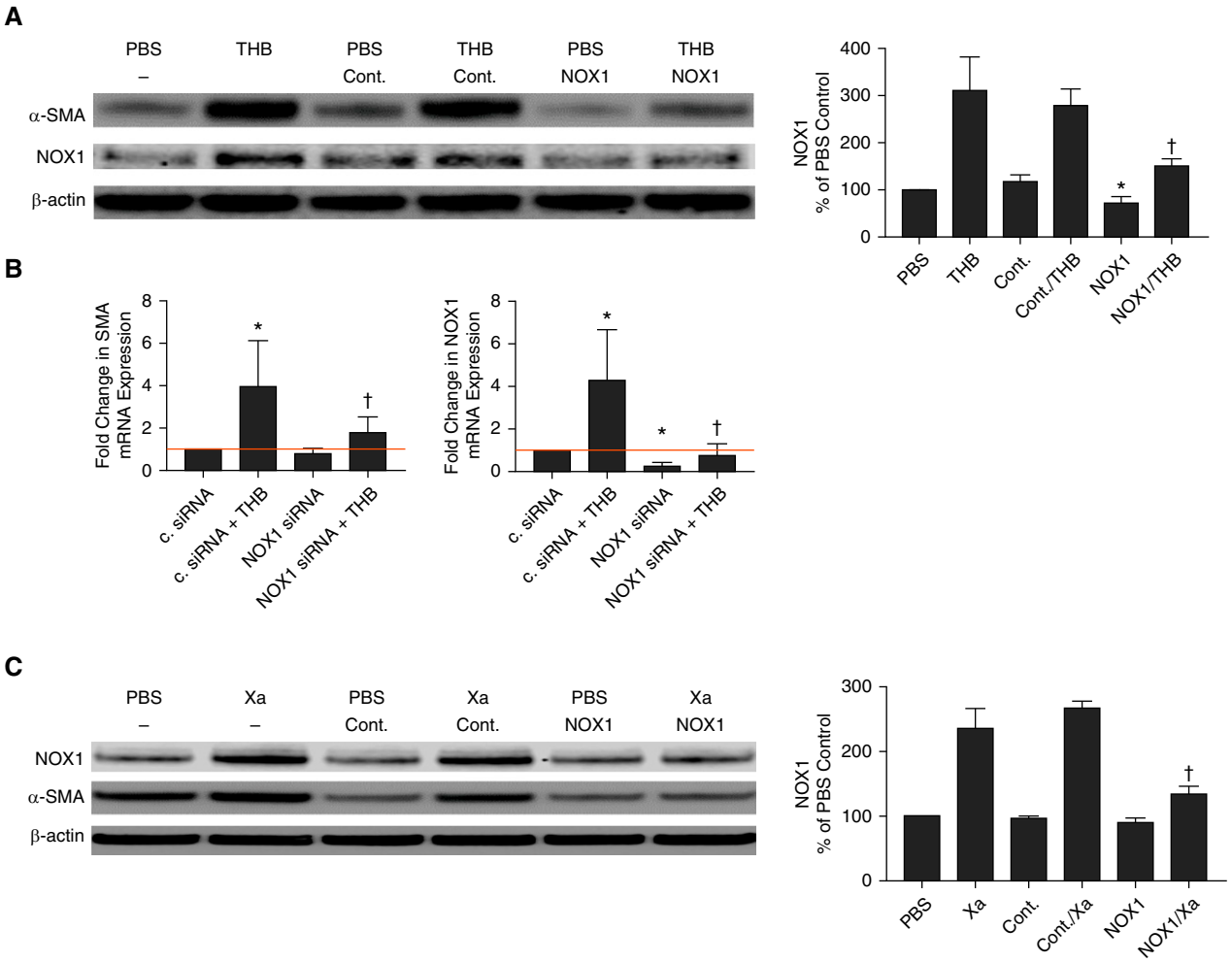

Figure 4. NOX1 downregulation attenuates THB- and Xa-induced MesoMT. Untransfected, c. siRNA–transfected, and NOX1 siRNA–transfected cells were serum starved for 24 hours. Cells were then treated with PBS or THB (7 nM) for 48 hours. (*A*) Cell lysates were resolved by SDS-PAGE and immunoblotted for α-SMA (α-smooth muscle actin) and NOX1 via Western blot. β-Actin was the loading Cont. The blots are representative of three independent experiments. Densitometrically derived data represent the mean of three independent experiments. (*B*) Total RNA was isolated from untransfected, c. siRNA–transfected, and NOX1 siRNA–transfected cells that had been treated with THB for 24 hours. Changes in α-SMA and NOX1 mRNA levels were determined by qPCR analyses. GUSB was used as the reference gene. Data represent the mean of three independent experiments. (*C*) Untransfected, c. siRNA–transfected, and NOX1 siRNA–transfected cells were serum starved for 24 hours. Cells were then treated with PBS or Xa (12 nM) for 48 hours. Cell lysates were resolved by SDS-PAGE and immunoblotted for α-SMA and NOX1 via Western blot. β-Actin was the loading Cont. The blots are representative of three independent experiments. Densitometrically derived data represent the mean of three independent experiments. $^{*}P < 0.05$ compared with c. siRNA and $^{\dagger}P < 0.05$ compared with c. siRNA–transfected cells treated with THB. Cont. or c. = control.

(12). However, TGF-β did not affect the expression of other NOX isoforms. Conversely, coagulation factors, Xa and THB, selectively induced NOX1 but had no effect on NOX4 expression. This finding is of particular relevance to pleural remodeling, as accelerated THB generation and coagulation are strongly implicated in the pathogenesis of pleural organization (8). Neither PLN nor uPA affected NOX expression in HPMCs. Although THB has been reported to induce NOX1 activity in a few prior studies, this is the first to show that NOX1 expression is enhanced in PMCs by THB and Xa. Furthermore, we found that NOX1 expression was enhanced in the pleura of patients with nonspecific pleuritis and in our mouse model of pleural empyema. This finding was supported by evidence of enhanced 4HNE detection, an indicator of significant ROS damage, in our murine empyema model. Although the role of ROS in the progression of PF remains to be fully defined, our data support the concept that NOX1 may contribute to outcomes in ROS-mediated pleural injury.

Because NOX1 was induced by Xa and THB, we first determined whether NOX1 contributed to Xa- and THB-mediated MesoMT. NOX1 downregulation significantly attenuated THB- and Xa-mediated induction of myofibroblast markers. These findings were confirmed with the NOX1 inhibitor ML-171. In pharmacologic-blockade analyses, the highest doses of ML-171 significantly reduced expression of the THB-mediated

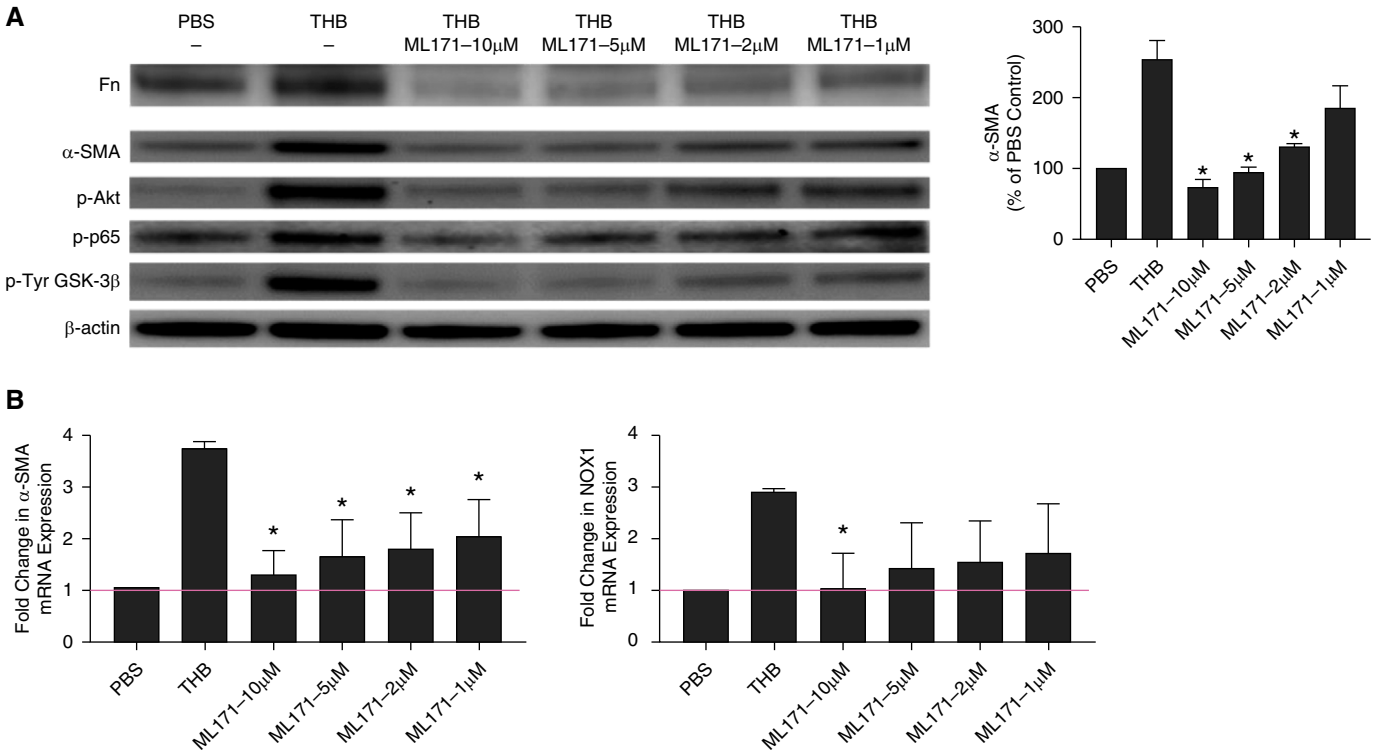

Figure 5. NOX1 inhibition with ML-171 blocks the induction of MesoMT. HPMCs were treated with varying doses of ML-171 (10–1 μM) in serum-free media for 24 hours before the addition of THB. Cells were then allowed to incubate for 48 hours. (*A*) Conditioned media and lysates were then resolved by SDS-PAGE and immunoblotted for fibronectin, α-SMA, and phosphor-Akt, -p65, and -GSK-3β by Western blot. β-Actin was the loading Cont. (*B*) For qPCR analyses, varying doses of ML-171 (10–1 μM) were added to cells, and then cells were allowed to incubate for 24 hours. THB was then added, and cells were incubated for 24 hours. Total RNA was then isolated and transcribed into cDNA. α-SMA and NOX1 expression were determined by qPCR analyses. GUSB served as the reference gene. The data represent the mean of three independent experiments. (*C*) HPMCs were treated with varying doses of ML-171 (10–1 μM) in serum-free media for 24 hours before the addition of Xa. Cells were then allowed to incubate for 48 hours. Conditioned media and lysates were then resolved by SDS-PAGE and immunoblotted for fibronectin, α-SMA, and phosphor-Akt, -p65, and -GSK-3β by Western blot. β-Actin was the loading Cont. (*D*) HPMCs were treated with varying doses of ML-171 (10–1 μM) in serum-free media for 24 hours before the addition of TGF-β. Cells were then allowed to incubate for 48 hours. Conditioned media and lysates were then resolved by SDS-PAGE and immunoblotted for collagen, α-SMA, and phosphor-Akt, -p65, and -GSK-3β by Western blot. β-Actin was the loading Cont. (*E*) For reversal studies, serum-starved HPMCs were treated with THB for 24 hours. Varying doses of ML-171 (5–1 μM) were then added to the THB-treated cells, and cells were allowed to incubate for 48 hours. Conditioned media and lysates were resolved by SDS-PAGE and immunoblotted for fibronectin, α-SMA, phosphorylated Akt, and p65. β-Actin was the loading Cont. The blots are representative of two independent experiments. *$P < 0.05$ compared with THB treatment. (*F*) For reactive oxygen species–generation studies, PBS- and ML-171–treated HPMCs were treated with Xa and THB. Cells were then incubated with 2′,7′-dichlorofluorescein (10 μM). Reactive oxygen species generation was visualized with a Bio-Rad ZOE fluorescent imager. Images show 20× magnification and are representative of the findings of six fields per well and three wells per group. Date represent three independent experiments. Scale bars, 100 μm. *$P < 0.05$ compared with untreated cells. Fn = fibronectin; ML-171 = NOX1 inhibitor; p-Tyr = phosphotyrosine.

MesoMT markers α-SMA and fibronectin. Furthermore, signaling pathways previously shown to be critical for the induction of MesoMT were attenuated in NOX1-inhibited cells. The inhibition of these signaling pathways and transcription factors likely contributed to the blockade of NOX1 induction by THB. Because the therapeutic targeting of NOX4 was shown to reverse pulmonary fibrosis *in vivo* (9), we evaluated ML-171 in *in vitro* reversal studies. In these studies, only the highest dose of ML-171 showed a modest effect on induction of fibronectin. Furthermore, the critical signaling pathways activated by THB (Akt and p65) that were attenuated in blockade studies remained active when ML-171 was used to reverse MesoMT. Although these data suggest that NOX1 plays a role in induction MesoMT, it remains possible that NOX4 may represent a more effective therapeutic target.

Previous studies have shown that byproducts of ROS, such as 4HNE and MDA, can propagate cellular signaling and injury independently of ROS (31–33). Our data here strongly suggest that NOX1-mediated ROS modifications, occurring before the use of an inhibitor, may be sufficient to propagate cellular signaling events necessary for the induction of MesoMT. These data are consistent with the lack of efficacy of antioxidant therapies for the treatment of other forms of pulmonary fibrosis (34). However, these data support our previous studies showing that inhibition of p65, PI3K/Akt, and GSK-3β signaling can reverse established MesoMT.

NOX4 is a constitutively active NOX, whose expression regulates its ability to produce the ROS H_2O_2. Although NOX4 is

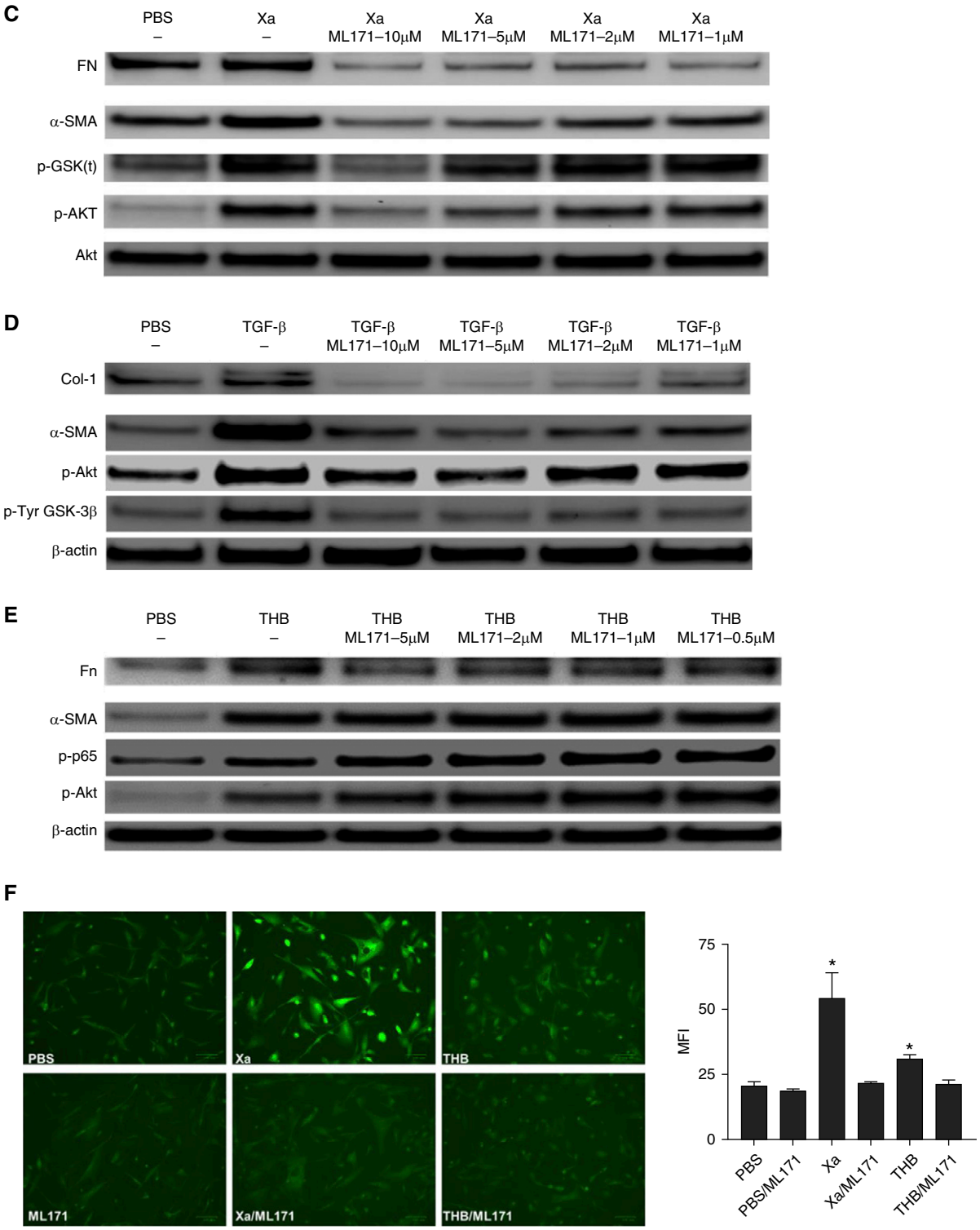

Figure 5. (*Continued*).

reported to be critical for TGF-β–mediated myofibroblast differentiation in other cell types, neither NOX4 nor NOX1 had, to our knowledge, been investigated in HPMCs. We found that NOX4 downregulation blocked TGF-β–mediated MesoMT and attenuated the activation of critical signaling pathways. These are the first studies to directly show that NOX4 downregulation attenuates this process in HPMCs. We also found that the effects of NOX1 downregulation and inhibition were not limited to THB, as TGF-β–mediated MesoMT was also blocked. There are numerous cytoplasmic subunits

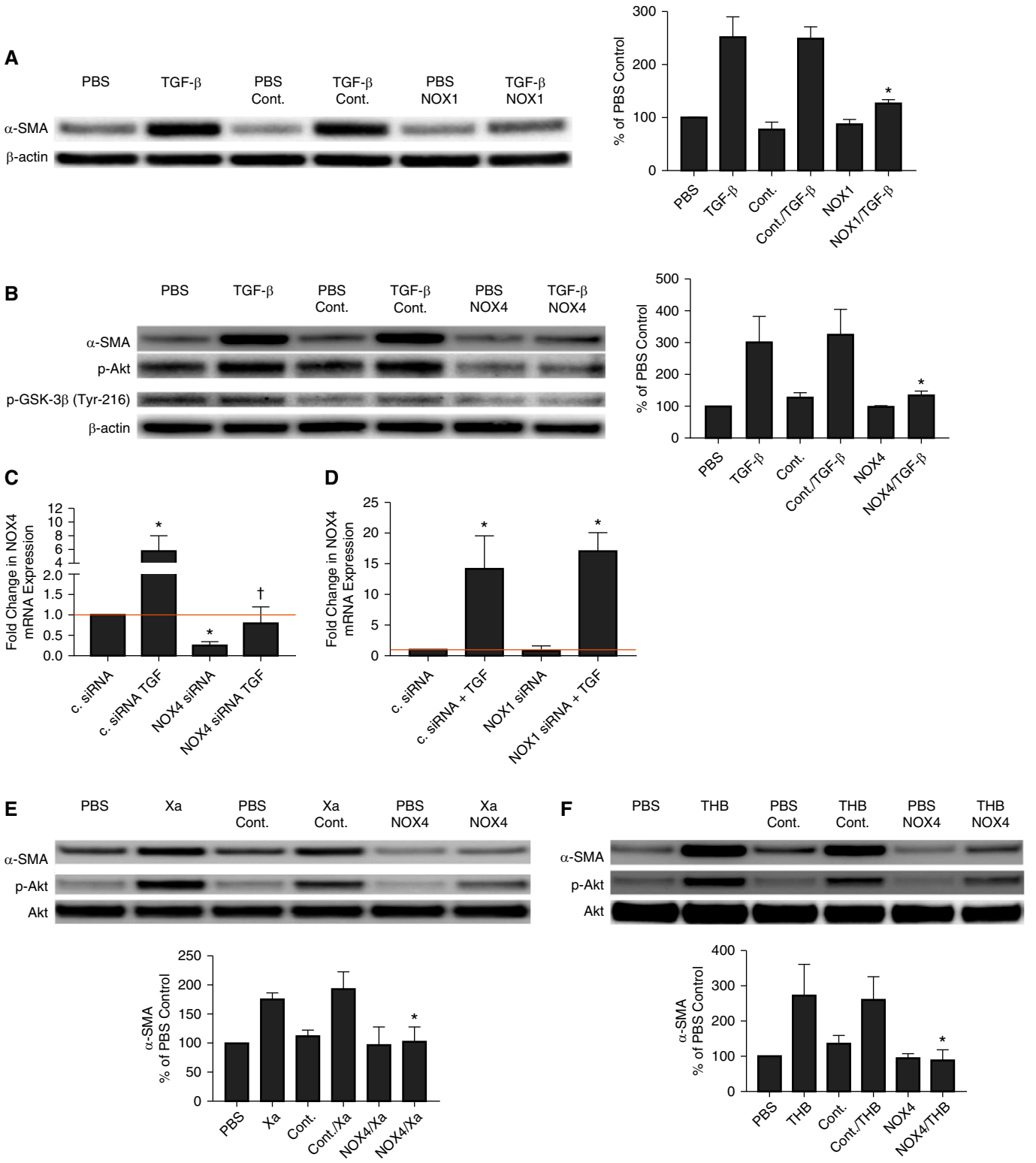

Figure 6. (*A–F*) NOX1 and NOX4 downregulation attenuates the induction of MesoMT by TGF-β. Untransfected, c. siRNA–transfected, and NOX1 (*A* and *D*) or NOX4 (*B–F*) siRNA–transfected cells were serum starved for 24 hours. Cells were then treated with PBS or TGF-β (5 ng/ml) for 24 hours or 48 hours. (*A*) Cell lysates were resolved by SDS-PAGE and immunoblotted for α-SMA via Western blot. β-Actin was the loading Cont. The blots are representative of three independent experiments. (*B*) Cell lysates were resolved by SDS-PAGE and immunoblotted for α-SMA, p-AKT, and pGSK3β via Western blot. β-Actin was the loading Cont. The blots are representative of three independent experiments. (*C*) Total RNA was isolated from c. siRNA– and NOX4 siRNA–transfected cells that had been treated with TGF-β for 24 hours. Changes in NOX4 mRNA levels were determined by qPCR analyses. GUSB was

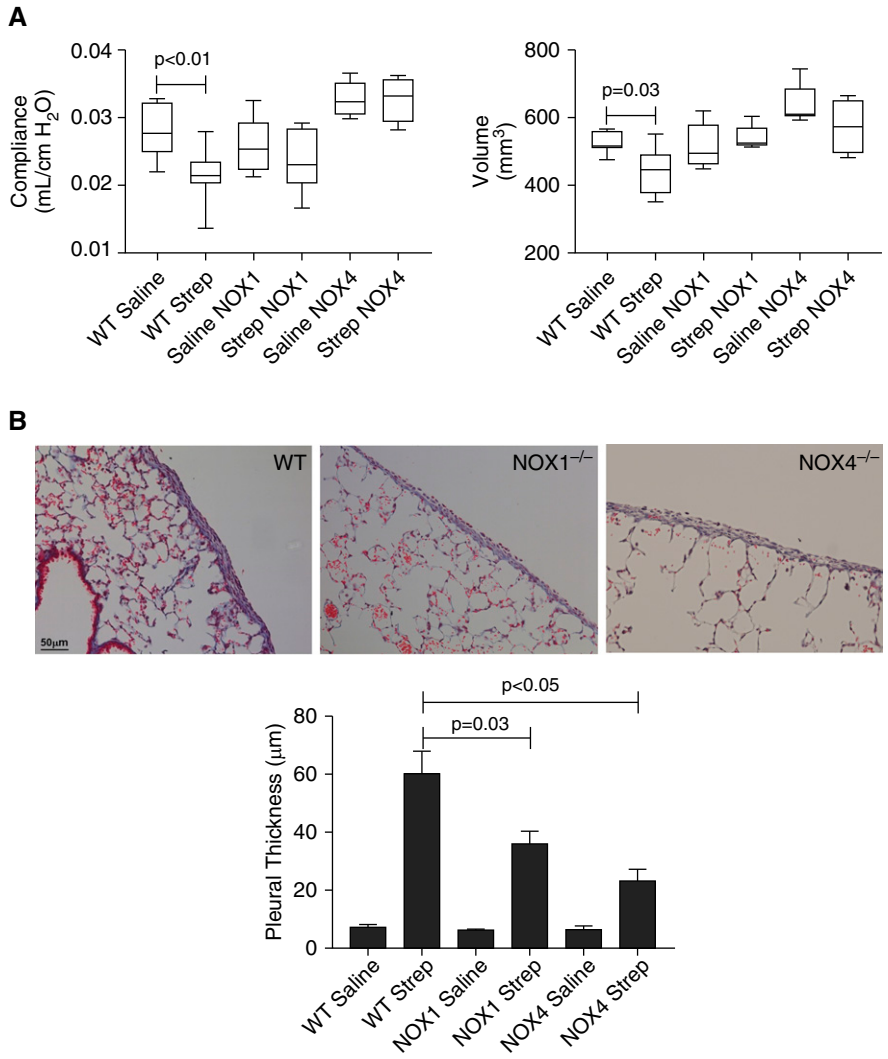

Figure 7. NOX1 and NOX4 deficiency attenuates the progression of empyema-mediated pleural fibrosis. Wild-type (WT), NOX1$^{-/-}$, and NOX4$^{-/-}$ mice were intrapleurally injected with 1.8×10^8 cfu of *Streptococcus pneumoniae*. After a 7-day time course, lung volumes and function were evaluated by a computed tomography scan and a SCIREQ flexiVent system, respectively. (*A*) NOX1 and NOX4 deficiency blocked significant *S. pneumoniae*–mediated decrements in lung volume and function. Tissue sections from *S. pneumoniae*–injured WT and NOX1-deficient mice were next Trichrome stained to characterize changes in lung architecture and collagen deposition. (*B*) *S. pneumoniae*–mediated pleural injury induced significant pleural thickening in WT mice compared with saline-treated WT mice. NOX1$^{-/-}$ and NOX4$^{-/-}$ mice demonstrated reduced pleural thickening compared with WT mice. $N = 5$–7 mice/group and 15 fields/slide. Strep = infected with *S. pneumoniae*. Scale bar, 50 μm.

involved in the regulation of NOX activity. NOX1 activation specifically requires association with p22, p67, and p47 (or their homologs NOXA1 and NOXO1, respectively), which may merit further investigation.

To evaluate the role of NOX1 and NOX4 in the progression of PF, we used our previously reported mouse empyema model (5, 6, 30). *S. pneumoniae*–mediated pleural injury was mitigated in NOX1- and NOX4-deficient mice. Furthermore, the significant pleural thickening demonstrated by the WT mice was significantly reduced in NOX1$^{-/-}$ and NOX4$^{-/-}$ mice. Although the significant decrements in lung function were partially blocked by NOX1 and NOX4 deficiency, residual pleural thickening persisted. These findings suggest that NOX1 and NOX4 contribute to the progression of PF. Furthermore, this process may involve a combination of factors, including synergistic NOX1 regulation of NOX4 activity or possible redundancy of the NOX-1 and -4 pathways. These areas merit continued investigation.

In summary, this report provides evidence for the important role of NOX1 in myofibroblast differentiation. Furthermore, previously unrecognized coagulation-pathway components, Xa and THB, are expressed in the setting of pleural inflammation, which contributes to florid fibrin deposition and tissue reorganization associated with pleural injury. TGF-β is likewise expressed locally in pleural injury and contributes to the process, in part through induction of MesoMT. Our findings suggest that induction of NOX1 and subsequent ROS generation could likewise contribute to MesoMT and ultimately PF. Although downregulation or inhibition of NOX1 can block the induction of MesoMT *in vitro*, our findings show that pharmacologic targeting of NOX1 *in vivo* may be difficult based on the inability of ML-171 to reverse established MesoMT *in vitro*. Alternative inhibitors may prove to be more effective and could emerge from future work to further define the mechanisms by which NOX1 inhibition protects against PF. Although TGF-β and other diverse factors drive myofibroblast differentiation in other cell types (6–8, 35, 36), our data delineate a novel contribution of NOX1 in the pathogenesis of both MesoMT and PF. ■

Author disclosures are available with the text of this article at www.atsjournals.org.

Figure 6. (*Continued*). used as the reference gene. (*D*) NOX1-downregulated cells were assayed for changes in NOX4 mRNA levels as determined by qPCR analyses. GUSB was used as the reference gene. Data represent the mean of three independent experiments. (*E–F*) Cells were then treated with PBS and Xa (*E*) or THB (*F*) for 48 hours. Cell lysates were resolved by SDS-PAGE and immunoblotted for α-SMA and phosphorylated Akt via Western blot. Total Akt was the loading Cont. Data are representative of three independent experiments. $^*P < 0.05$ compared with c. siRNA and $^\dagger P < 0.05$ compared with the TGF-β–treated c. siRNA.

References

1. Huggins JT, Sahn SA. Causes and management of pleural fibrosis. *Respirology* 2004;9:441–447.
2. Lee YC, Vaz MA, Ely KA, McDonald EC, Thompson PJ, Nesbitt JC, *et al*. Symptomatic persistent post-coronary artery bypass graft pleural effusions requiring operative treatment: clinical and histologic features. *Chest* 2001;119:795–800.
3. Jantz MA, Antony VB. Pleural fibrosis. *Clin Chest Med* 2006;27:181–191.
4. Heffner JE, Klein JS, Hampson C. Interventional management of pleural infections. *Chest* 2009;136:1148–1159.
5. Boren J, Shryock G, Fergis A, Jeffers A, Owens S, Qin W, *et al*. Inhibition of glycogen synthase kinase 3β blocks mesomesenchymal transition and attenuates *Streptococcus* pneumonia-mediated pleural injury in mice. *Am J Pathol* 2017;187:2461–2472.
6. Tucker TA, Jeffers A, Boren J, Quaid B, Owens S, Koenig KB, *et al*. Organizing empyema induced in mice by *Streptococcus pneumoniae*: effects of plasminogen activator inhibitor-1 deficiency. *Clin Transl Med* 2016;5:17.
7. Owens S, Jeffers A, Boren J, Tsukasaki Y, Koenig K, Ikebe M, *et al*. Mesomesenchymal transition of pleural mesothelial cells is PI3K and NF-κB dependent. *Am J Physiol Lung Cell Mol Physiol* 2015;308: L1265–L1273.
8. Tucker TA, Jeffers A, Alvarez A, Owens S, Koenig K, Quaid B, *et al*. Plasminogen activator inhibitor-1 deficiency augments visceral mesothelial organization, intrapleural coagulation, and lung restriction in mice with carbon black/bleomycin-induced pleural injury. *Am J Respir Cell Mol Biol* 2014;50:316–327.
9. Hecker L, Logsdon NJ, Kurundkar D, Kurundkar A, Bernard K, Hock T, *et al*. Reversal of persistent fibrosis in aging by targeting Nox4-Nrf2 redox imbalance. *Sci Transl Med* 2014;6:231ra47.
10. Ding Q, Luckhardt T, Hecker L, Zhou Y, Liu G, Antony VB, *et al*. New insights into the pathogenesis and treatment of idiopathic pulmonary fibrosis. *Drugs* 2011;71:981–1001.
11. Hecker L, Vittal R, Jones T, Jagirdar R, Luckhardt TR, Horowitz JC, *et al*. NADPH oxidase-4 mediates myofibroblast activation and fibrogenic responses to lung injury. *Nat Med* 2009;15:1077–1081.
12. Zolak JS, Jagirdar R, Surolia R, Karki S, Oliva O, Hock T, *et al*. Pleural mesothelial cell differentiation and invasion in fibrogenic lung injury. *Am J Pathol* 2013;182:1239–1247.
13. Cuzzocrea S, McDonald MC, Filipe HM, Costantino G, Mazzon E, Santagati S, *et al*. Effects of tempol, a membrane-permeable radical scavenger, in a rodent model of carrageenan-induced pleurisy. *Eur J Pharmacol* 2000;390:209–222.
14. Altenhöfer S, Radermacher KA, Kleikers PW, Wingler K, Schmidt HH. Evolution of NADPH oxidase inhibitors: selectivity and mechanisms for target engagement. *Antioxid Redox Signal* 2015;23:406–427.
15. Panday A, Sahoo MK, Osorio D, Batra S. NADPH oxidases: an overview from structure to innate immunity-associated pathologies. *Cell Mol Immunol* 2015;12:5–23.
16. Brown DI, Griendling KK. Nox proteins in signal transduction. *Free Radic Biol Med* 2009;47:1239–1253.
17. Li FJ, Duggal RN, Oliva OM, Karki S, Surolia R, Wang Z, *et al*. Heme oxygenase-1 protects corexit 9500A-induced respiratory epithelial injury across species. *PLoS One* 2015;10:e0122275.
18. Jiang F, Liu GS, Dusting GJ, Chan EC. NADPH oxidase-dependent redox signaling in TGF-β-mediated fibrotic responses. *Redox Biol* 2014;2:267–272.
19. Zhang Y, Zhang X, Rabbani ZN, Jackson IL, Vujaskovic Z. Oxidative stress mediates radiation lung injury by inducing apoptosis. *Int J Radiat Oncol Biol Phys* 2012;83:740–748.
20. Barnes JL, Gorin Y. Myofibroblast differentiation during fibrosis: role of NAD(P)H oxidases. *Kidney Int* 2011;79:944–956.
21. Cucoranu I, Clempus R, Dikalova A, Phelan PJ, Ariyan S, Dikalov S, *et al*. NAD(P)H oxidase 4 mediates transforming growth factor-beta1-induced differentiation of cardiac fibroblasts into myofibroblasts. *Circ Res* 2005;97:900–907.
22. Ghatak S, Hascall VC, Markwald RR, Feghali-Bostwick C, Artlett CM, Gooz M, *et al*. Transforming growth factor β1 (TGFβ1)-induced CD44V6-NOX4 signaling in pathogenesis of idiopathic pulmonary fibrosis. *J Biol Chem* 2017;292:10490–10519.
23. Jagadeesha DK, Takapoo M, Banfi B, Bhalla RC, Miller FJ Jr. Nox1 transactivation of epidermal growth factor receptor promotes N-cadherin shedding and smooth muscle cell migration. *Cardiovasc Res* 2012;93:406–413.
24. Gavazzi G, Banfi B, Deffert C, Fiette L, Schappi M, Herrmann F, *et al*. Decreased blood pressure in NOX1-deficient mice. *FEBS Lett* 2006; 580:497–504.
25. Williams L, Tucker TA, Koenig K, Allen T, Rao LV, Pendurthi U, *et al*. Tissue factor pathway inhibitor attenuates the progression of malignant pleural mesothelioma in nude mice. *Am J Respir Cell Mol Biol* 2012;46:173–179.
26. Tucker TA, Williams L, Koenig K, Kothari H, Komissarov AA, Florova G, *et al*. Lipoprotein receptor-related protein 1 regulates collagen 1 expression, proteolysis, and migration in human pleural mesothelial cells. *Am J Respir Cell Mol Biol* 2012;46:196–206.
27. Kamata H, Tsukasaki Y, Sakai T, Ikebe R, Wang J, Jeffers A, *et al*. KIF5A transports collagen vesicles of myofibroblasts during pleural fibrosis. *Sci Rep* 2017;7:4556.
28. Idell S, Zwieb C, Kumar A, Koenig KB, Johnson AR. Pathways of fibrin turnover of human pleural mesothelial cells *in vitro*. *Am J Respir Cell Mol Biol* 1992;7:414–426.
29. Jeffers A, Owens S, Koenig K, Quaid B, Pendurthi UR, Rao VM, *et al*. Thrombin down-regulates tissue factor pathway inhibitor expression in a PI3K/nuclear factor-κB-dependent manner in human pleural mesothelial cells. *Am J Respir Cell Mol Biol* 2015;52: 674–682.
30. Tucker T, Tsukasaki Y, Sakai T, Mitsuhashi S, Komatsu S, Jeffers A, *et al*. Myocardin is involved in mesothelial-mesenchymal transition of human pleural mesothelial cells. *Am J Respir Cell Mol Biol* 2019;61: 86–96.
31. Kwiecien S, Jasnos K, Magierowski M, Sliwowski Z, Pajdo R, Brzozowski B, *et al*. Lipid peroxidation, reactive oxygen species and antioxidative factors in the pathogenesis of gastric mucosal lesions and mechanism of protection against oxidative stress-induced gastric injury. *J Physiol Pharmacol* 2014;65:613–622.
32. Yang Y, Sharma R, Sharma A, Awasthi S, Awasthi YC. Lipid peroxidation and cell cycle signaling: 4-hydroxynonenal, a key molecule in stress mediated signaling. *Acta Biochim Pol* 2003;50: 319–336.
33. Dwivedi S, Sharma A, Patrick B, Sharma R, Awasthi YC. Role of 4-hydroxynonenal and its metabolites in signaling. *Redox Rep* 2007;12:4–10.
34. Kandhare AD, Mukherjee A, Ghosh P, Bodhankar SL. Efficacy of antioxidant in idiopathic pulmonary fibrosis: a systematic review and meta-analysis. *EXCLI J* 2016;15:636–651.
35. Lan A, Qi Y, Du J. Akt2 mediates TGF-β1-induced epithelial to mesenchymal transition by deactivating GSK3β/snail signaling pathway in renal tubular epithelial cells. *Cell Physiol Biochem* 2014; 34:368–382.
36. Kalluri R, Neilson EG. Epithelial-mesenchymal transition and its implications for fibrosis. *J Clin Invest* 2003;112:1776–1784.